

Effect of co-existing crystal structures on magnetic properties of $\text{Ni}_2\text{Mn}_{1+x}\text{Sn}_{1-x}$ magnetic shape memory alloy

Soumyadip Pal,^{1,2} Sandeep Singh,¹ and Chhayabrita Maji^{1,3, a)}

¹⁾Department of Condensed Matter Physics and Material Sciences, S N Bose National Centre for Basic Sciences, Block-JD, Sector-III, Salt Lake, Kolkata - 700106, West Bengal, India.

²⁾Department of Physics, Calcutta Institute of Technology, Banitabla, Uluberia, Howrah - 711316, West Bengal, India.

³⁾Department of Materials Science, Indian Association for the Cultivation of Science, 2A & 2B Raja S.C. Mullick Road, Jadavpur, Kolkata - 700032, West Bengal, India.

The $\text{Ni}_2\text{Mn}_{1+x}\text{Sn}_{1-x}$ ($x = 0.4$ and 0.44) magnetic shape memory alloys exhibit magnetic field induced shift of martensitic transition to lower temperature with applications in magnetic refrigeration, magnetic actuators, and magnetic sensors. To significantly improve the understanding of material properties for applications, the temperature dependent crystal structure analysis is associated with the magnetic properties alongwith theoretical calculations that probed the cause of spin-glass like behavior and shift of martensitic transition to lower temperature with magnetic field. Furthermore, it is found that the martensitic transition in $x = 0.52$ occurs without spin-lattice coupling.

PACS numbers: 61.05.cp, 61.66.Dk, 75.20.En, 75.50.Cc

The new class of off-stoichiometric magnetic shape memory alloys (MSMA) that exhibit shift of martensitic transition (ΔM_s) to lower temperature with applied magnetic field has gained adequate scientific attention due to shift induced attractive properties like giant magnetocaloric effects¹, giant magneto-resistance², magnetic shape memory effects³ and exchange bias effects⁴. These fascinating properties make the alloys a potential candidate for applications in solid-state magnetic refrigeration¹, magnetic actuators⁵ and magnetic sensors² etc. This class of material are very important for replacing present way of cooling with hazardous gases. These MSMA exhibit giant magnetocaloric effect, also, with applied pressure that are comparable to reported present material for solid-state refrigeration⁶. Moreover, these alloys offer cost effective technology.

In contrary to the Ni_2MnGa and off-stoichiometric Ni-Mn-Ga, the application of magnetic field shifts the martensitic transition to lower temperatures in $\text{Ni}_2\text{Mn}_{1+x}\text{Sn}_{1-x}$ (NiMnSn), $\text{Ni}_2\text{Mn}_{1+x}\text{In}_{1-x}$ (NiMnIn) and $\text{Ni}_{2-y}\text{Co}_y\text{Mn}_{1+x}\text{In}_{1-x}$ (NiCoMnIn). However, the ΔM_s differs with composition. The $\Delta M_s/\Delta H$ for NiMnSn, NiMnIn and NiCoMnIn are ~ -1.5 K/Tesla⁷, ~ -12 K/Tesla⁸, ~ -10 K/Tesla⁹, respectively. The large ΔM_s in NiMnIn gives rise to giant magnetocaloric effect and giant magnetoresistance as compared to that of NiMnSn and NiCoMnIn. A thermodynamical framework⁵ explains that Zeman energy and magnetocrystalline anisotropy energies differences of the austenitic and martensitic phases determine the effect of the applied magnetic field on phase transformation. If the saturation magnetization of austenite is higher than

the saturation magnetization of martensitic phase (MP) in case of NiMnZ (Z as In, Sn, or Sb), the magnetic field favors austenite resulting in austenitic phase stabilization and a decrease in transformation temperatures⁵. The ac susceptibility as a function of frequency shows that NiMnSn behaves as re-entrant spin-glass system¹⁰.

In this letter, the crystal structure changes as a function of temperature in $\text{Ni}_2\text{Mn}_{1+x}\text{Sn}_{1-x}$ ($x = 0.40, 0.44$, and 0.52) alloys are investigated till 10 K. The behavior of crystal structure explains the magnetic changes. The coupling between spin and lattice is established. The cause of re-entrant spin-glass-like behavior and ΔM_s is found. In addition, the $x = 0.52$ composition that does not exhibit ΔM_s but undergoes martensitic transition is also probed. It is reported that the martensitic transition occurs due to spin-lattice coupling¹¹. The result for $x = 0.52$ shows that martensitic transition occurs in absence of spin-lattice coupling also.

The polycrystalline ingots of $\text{Ni}_2\text{Mn}_{1+x}\text{Sn}_{1-x}$ ($x = 0.40, 0.44, 0.48$ and 0.52) alloys are prepared by arc melting appropriate amount of high purity ($\geq 99.99\%$) constituent elements under argon atmosphere and were annealed at 1173 K (24 h) with subsequent quenching to ice water. The alloys are characterized as mentioned in Ref. 2. The structural and magnetic transition temperatures are determined by differential scanning calorimetry (DSC) measurements. The values of the transition temperatures are tabulated in Ref. 2. Below room temperature, $x = 0.40$ and 0.44 transform from ferromagnetic austenitic phase (AP) to mixed magnetic martensitic phase (MP) where co-existence of ferromagnetic (FM) and antiferromagnetic (AFM) coupling is reported¹²⁻¹⁵, whereas $x = 0.48$ and 0.52 transform from paramagnetic AP to paramagnetic MP and consequently to mixed magnetic MP. In these systems the doped Mn at Sn site (Mn2) are antiferromagnetically coupled to Ni

^{a)}Email: chhayabrita@gmail.com; Corresponding author; Previous publication name: C.Biswas

and original Mn (Mn1)^{12–15}, whereas Mn1 is ferromagnetically coupled to Ni. The temperature dependent X-ray diffraction (XRD) measurements are performed using synchrotron radiation of energy 18 KeV from room temperature to 10 K at Indian Beam line, Photon factory, KEK, Japan.

The magnetic exchange parameter (J) between first nearest neighbour Mn1-Mn2 of 16 atom unit cell of $x = 0.5$ is calculated using experimentally obtained lattice parameters at different temperatures of $x = 0.44$ on the basis of the idea of ising model where the energy of any spin system can be described by $E = - \sum_{i \neq j} J_{ij} S_i S_j$.

The *ab initio* calculations are performed using the PAW method as implemented in the VASP¹⁶ code within GGA for the exchange correlation functional. Monkhorst-Pack k-points mesh of $10 \times 10 \times 10$ was used for calculation.

The LeBail fitting of temperature dependent XRD patterns of $x = 0.44$ and 0.52 are shown in fig. 1. It is noteworthy that MP has two co-existing orthorhombic structures, namely, 4-layered (4L) and 14-layered (14L) with space group $Pmma$. The rest of the compositions $x = 0.4$ and 0.48 also show co-existence of 4L and 14L structures in MP. The mixture of two structures in MP

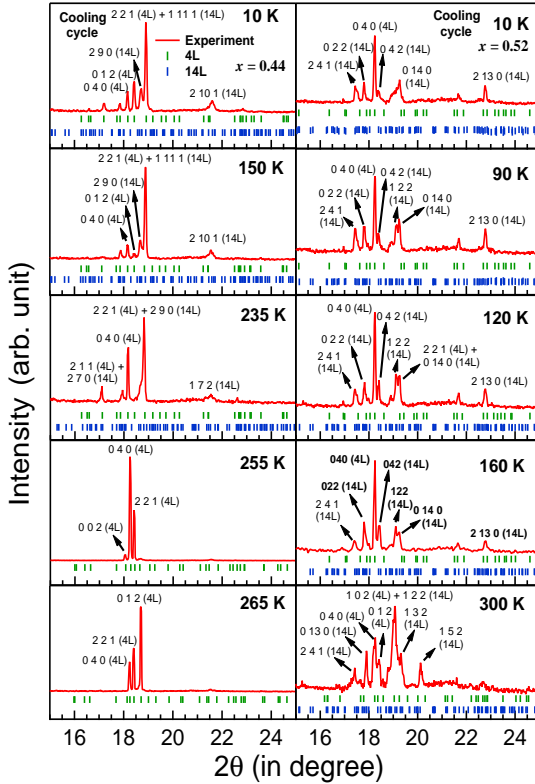


FIG. 1. Temperature variation of X-ray diffraction indexed by co-existing 4-layered and 14-layered orthorhombic crystal structure of $x = 0.44$ and 0.52 .

is, also, found in other Heusler alloys^{17–19}. The AP has $L2_1$ cubic structure². The transformation from $L2_1$ cubic

to 4L and 14L takes place by contraction along c -axis and elongation along b -axis according to Bain transformation.

Interestingly, the phase fraction of co-existing 4L and 14L structure varies as a function of temperature. The Fig. 2 shows the phase fraction percentage of $L2_1$, 4L and 14L as a function of temperature for $x = 0.40$ and 0.44 . Upon martensitic transition, initially, cubic $L2_1$ structure

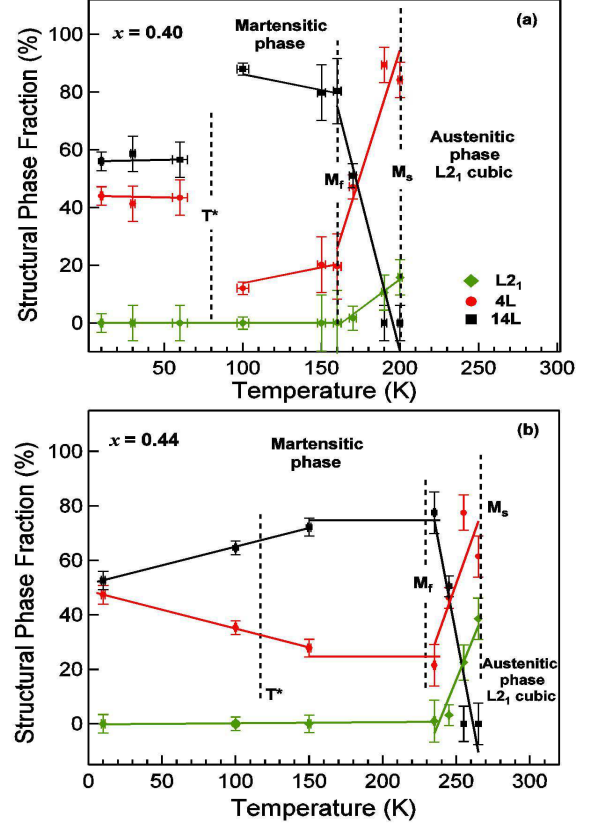


FIG. 2. (a) and (b) 4-layered and 14-layered structural phase fraction variation in martensitic transition region, martensitic phase, and below T^* region of $x = 0.40$ and 0.44 , respectively.

transforms to 4L structure. In between martensitic start (M_s) and martensitic finish (M_f) temperature range the 14L structure evolves at the cost of 4L phase. Between M_f and spin freezing temperature T^* (referred as T_f in Ref. 10) the phase fraction is almost constant. Noteworthy, below T^* the 4L phase fraction increases and 14L phase fraction decreases. The phase fraction of 4L and 14L is around 50 % at 10 K. The intermartensitic transition is reported earlier for NiMnGa²⁰, NiMnGaFe²¹ and NiMnIn alloys²². The stability of the MP is achieved by transition to either 14L (7M) or non-modulated structure mainly through 10M structure. For present NiMnSn alloys the martensitic transition to 14L structure is happening through 4L structure. For $Ni_2Mn_{1.44}Sn_{0.56}$ the transition from $L2_1$ to 4L is reported earlier¹⁵.

The formation energy per unit cell of 4L and 14L structures is calculated using experimental lattice constants of 14L and 4L structures at 150 K and 190 K, respectively,

by *ab initio* density functional theory. The formation energy per unit cell of 4L (-1.040315 eV) and 14L (-1.023121 eV) are very close to each other but 4L requires less formation energy than 14L. Thus, initially, the martensitic transformation from parent phase to 4L structure occurs. To accommodate the stress accumulation by 4L structure, the transition to stacking sequence 14L occurs. This internal stress-related selectivity of intermartensitic transformation was also confirmed in other systems^{23–25}. Since 4L is more favorable structure because it requires less formation energy than 14L, the 80% phase fraction of 14L induces instability in the MP. Hence, to minimize the free energy of the system, the phase fraction of 4L structure increases once more. It is very important to note that the change in phase fraction of 4L and 14L occurs at the temperatures where magnetic phase change also occurs. The thermo magnetization behavior for $x = 0.40$ and $x = 0.44$ is shown in Ref. 2, and Ref. 25, respectively.

In NiMnSn off-stoichiometric alloys the bond distance between Mn1 and Mn2 gives rise to the antiferromagnetism¹. Thus, the bond distance between Mn1-Mn2 is deduced from the structural analysis and exchange integral between Mn1-Mn2 ($J_{Mn1-Mn2}$) is calculated as a function of temperature (Fig. 3). The cal-

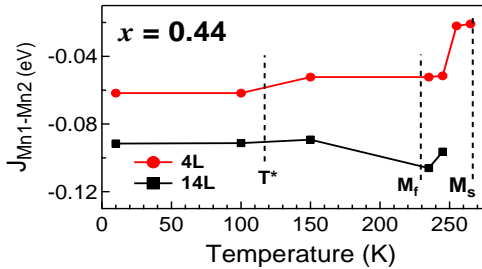


FIG. 3. Calculated magnetic exchange coupling constant (J) between first nearest neighbours Mn1-Mn2 of $x = 0.50$ using experimentally obtained lattice parameters of $x = 0.44$.

ulation shows that AFM exchange interaction exists between Mn1-Mn2 in both 4L and 14L structures. Also, the AFM exchange interaction is more strong in 14L than 4L. Thus, presence of two structural phases with different strength of exchange interaction gives rise to magnetically inhomogeneous phase. Also, the resistivity analysis under ZFC and FC reveals that short-range anti-ferromagnetism exists²⁶. Moreover, it is known that the low temperature phase consists of various martensitic variants oriented in different directions derived from high symmetry cubic phase²⁷. Thus, the variants of orthorhombic 4L and 14L evolves randomly oriented. With almost equal phase fraction of 4L and 14L, random orientation of their variants, co-existence of FM and AFM coupling, short-range AFM coupling, and different strength of AFM coupling might pin the FM moments by exchange bias to AFM spin moments. A diffuse AFM phase starts

to develop below M_s and becomes strong enough below T^* (or T_f) to cause the spin freezing¹⁰. Thus, the re-entrant spin-glass like magnetic phase is obtained as reported in Ref. 10.

The $x = 0.52$ composition does not show magnetic field induced shift of martensitic transition to lower temperature. However, it undergoes reversible martensitic transition as shown in fig. 4. The M_s and M_f of $x = 0.52$ are

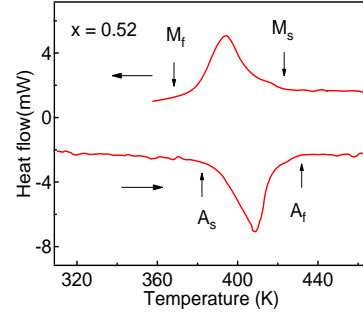


FIG. 4. For $x = 0.52$, the exothermic (cooling) and endothermic (heating) behavior observed by differential scanning calorimetry.

416 and 378 K, respectively. However, the martensitic Curie temperature is 175 K. Thus, within martensitic phase there is paramagnetic to ferromagnetic transition. The phase fraction of 14L is more than 4L, similar to 0.40 and 0.44. The structural phase fraction (4L \approx 30 % and 14L \approx 70 %) remains almost unchanged over the observed temperature range as evident from Fig. 5 (a), whereas, the magnetization decreases. That means there is a spin reorientation even in martensitic phase. The corresponding structural changes do not follow magnetization change as a function of temperature (Fig. 5 (a) and (b)). This implies that spin-lattice coupling is absent in $x = 0.52$. Hence, the martensitic transition occurs without spin-lattice coupling.

In the martensitic phase the co-existence of two crystal structures, change in crystal structure phase fraction with magnetic transition, spin-lattice coupling, and co-existence of ferromagnetic and anti-ferromagnetic magnetic phase with different strength of AFM coupling gives rise to structurally and magnetically disordered martensitic phase that causes spin-glass-like behavior of $Ni_2Mn_{1+x}Sn_{1-x}$ ($x = 0.4, 0.44, 0.48$ and 0.52). Also, due to these reasons the saturation magnetization of MP decreases favoring stability of austenitic phase according to thermodynamical model⁵. Thus, with application of magnetic field the spins might orient to more ordered state favoring retention of cubic $L2_1$ crystal structure through spin-lattice coupling. Hence, martensitic transition shifts to lower temperature. The martensitic transition in $x = 0.52$ occurs without spin-lattice coupling. These results call for similar investigation of other magnetic shape memory alloys exhibiting shift of martensitic transition to lower temperature with applied magnetic

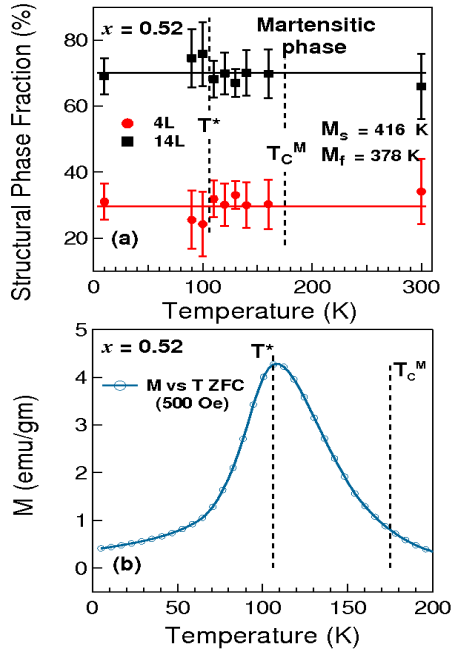


FIG. 5. For $x=0.52$, the structural phase fraction (a) and zero-field-cooled thermo-magnetization (b) variation in martensitic phase and below T^* .

field. Also, the microscopic origin needs to be probed.

We would like to thank DST-KEK for financial assistance to do experiment in Photon factory. We also wish to thank Dr. M. K. Mukhopadhyay and Mr. Satish Poddar for their help during experiment. We appreciate the support of Prof. Priya Mahadevan for VASP calculation. Prof. B. N. Dev and Prof. G. P. Das are acknowledged for fruitful discussion.

REFERENCES

- ¹T. Krenke, E. Duman, M. Acet, E. F. Wassermann, X. Moya, L. Mañosa, and A. Planes, *Nat. Mater.* **4**, 450 (2005).
- ²S. Singh and C. Biswas, *Appl. Phys. Lett.* **98**, 212101 (2011).
- ³R. Kainuma, Y. Imano, W. Ito, Y. Sutou, H. Morito, S. Okamoto, O. Kita-kami, K. Oikawa, A. Fujita, T. Kanomata, and K. Ishida, *Nature (London)* **493**, 957 (2006).
- ⁴B. M. Wang, Y. Liu, P. Ren, B. Xia, K. B. Ruan, J. B. Yi, J. Ding, X. G. Li, and L. Wang, *Phys. Rev. Lett.* **106**, 077203 (2011).
- ⁵H. E. Karaca, I. Karaman, B. Basaran, Y. Ren, Y. I. Chumlyakov, and H. J. Maier, *Adv. Funct. Mater.* **19**, 983 (2009).
- ⁶Llus Maosa, David Gonzlez-Alonso, Antoni Planes, Errell Bonnot, Maria Barrio, Josep-Llus Tamarit, Seda Aksoy and Mehmet Acet, *Nat. Mater.* **9**, 478 (2010).

- ⁷P. J. Shamberger and F. S. Ohuchi, *Phys. Rev. B* **79**, 144407 (2009).
- ⁸S. Singh, I. Glavatsky, and C. Biswas, *J. Alloys Compd.* **615**, 994 (2014).
- ⁹V. Recarte, J. I. Pérez-Landazúbal, S. Kustov, and E. Cesari, *J. Appl. Phys.* **107**, 053501 (2010).
- ¹⁰S. Chatterjee, S. Giri, S. K. De, and S. Majumdar, *Phys. Rev. B* **79**, 092410 (2009).
- ¹¹S. B. Roy, *J. Phys.: Condens. Matter* **25**, 183201 (2013).
- ¹²S. Pal, P. Mahadevan, and C. Biswas, *AIP Conf. Proc.* **1591**, 58 (2014).
- ¹³M. Ye, A. Kimura, Y. Miura, M. Shirai, Y. T. Cui, K. Shimada, H. Namatame, M. Taniguchi, S. Ueda, K. Kobayashi, R. Kainuma, T. Shishido, K. Fukushima, and T. Kanomata, *Phys. Rev. Lett.* **104**, 176401 (2010).
- ¹⁴T. Kanomata, K. Fukushima, H. Nishihara, R. Kainuma, W. Ito, K. Oikawa, K. Ishida, K. U. Neumann, and K. R. A. Ziebeck, *Mater. Sci. Forum* **583**, 119 (2008).
- ¹⁵P. J. Brown, A. P. Gandy, K. Ishida, R. Kainuma, T. Kanomata, K. -U. Neumann, K. Oikawa, B. Ouladdiaf, and K. R. A. Ziebeck, *J. Phys.: Condens. Matter* **18**, 2249 (2006).
- ¹⁶G. Kresse and J. Furthmüller, *Phys. Rev. B* **54**, 11169 (1996).
- ¹⁷K. Oikawa, W. Ito, Y. Imano, Y. Sutou, R. Kainuma, K. Ishida, S. Okamoto, O. Kitakami, and T. Kanomata, *Appl. Phys. Lett.* **88**, 122507 (2006).
- ¹⁸V. V. Khovaylo, T. Kanomata, T. Tanaka, M. Nakashima, Y. Amako, R. Kainuma, R. Y. Umetsu, H. Morito, and H. Miki, *Phys. Rev. B* **80**, 144409 (2009).
- ¹⁹W. Ito, Y. Imano, R. Kainuma, Y. Sutou, K. Oikawa, and K. Ishida, *Metall. Mater. Trans. A* **38**, 759 (2007).
- ²⁰C. Seguí, E. Cesari, and J. Pons, *Adv. Mater. Res.* **52**, 47 (2008).
- ²¹K. Koho, O. Söderberg, N. Lanska, Y. Ge, X. Liu, L. Straka, J. Vimpri, O. Heczko, and V.K. Lindroos, *Mat. Sci. Eng. A* **378**, 384 (2004).
- ²²Y. J. Huang, Q. D. Hu, J. Liu, L. Zeng, D. F. Zhang, and J. G. Li, *Acta Mater.* **61**, 5702 (2013).
- ²³W. H. Wang, Z. H. Liu, J. Zhang, J. L. Chen, G. H. Wu, W. S. Zhan, T. S. Chin, G. H. Wen, and X. X. Zhang, *Phys. Rev. B* **66**, 052411 (2002).
- ²⁴C. Seguí, J. Pons, and E. Cesari, *Acta Mater.* **55**, 1649 (2007).
- ²⁵R. F. Hamilton, H. Sehitoglu, C. Efstathiou, and H. J. Maier, *Acta Mater.* **55**, 4867 (2007).
- ²⁶Sandeep Singh, Soumyadipta Pal, and C. Biswas, *J. Alloys and Compounds* **616**, 110 (2014).
- ²⁷H. Zheng, W. Wang, S. Xue, Q. Zhai, J. Frenzel, and Z. Luo, *Acta Mater.* **61**, 4648 (2013).